

Wow defect reduction based on interpolation techniques

P. MAZIEWSKI*

Multimedia Systems Department, Gdańsk University of Technology, 11/12 Narutowicza St., 80-952 Gdańsk, Poland

Abstract. In this paper the capacity of non-uniform sampling rate conversion techniques, involving different interpolation methods, aimed at wow defect reduction, is examined. Involved are: linear interpolation, four polynomial-based interpolation methods and the windowed sinc-based method. The examined polynomial methods are: Lagrange interpolation, polynomial fitting with additional noise reduction, Hermitan and Spline. The performance of an artificially distorted audio signal, restored using non-uniform resampling, is evaluated on the basis of standard audio defect measurement criteria and compared for all of the aforementioned interpolation methods. The chosen defect descriptors are: total harmonic distortion, total harmonic distortion plus noise and signal to noise ratio.

Key words: Wow defect reduction, audio signal restoration, linear interpolation, polynomial interpolation, sinc-based interpolation, non-uniform sampling rate conversion.

1. Introduction

The preservation of mechanically and magnetically recorded sound is an issue of considerable current interest. Extensive recorded sound collections and archives exist world-wide. Normally, in sound recording, it is impossible to obtain absolutely constant speed of the recording medium because of the limited precision of the mechanical drive. This concerns especially old recordings. As a result different forms of distortions arise caused by an irregular motion of the recording medium during the recording, duplicating and reproducing processes. Among them a wow defect appears, which is especially difficult to cancel.

As mentioned above, the main source of the wow defect is the variable velocity of the sound conveyer. The reasons for this can be different. One origin can be found in the eccentricity or ellipticity of the audio equipment mechanical parts and the conveyer itself [1]. It is a frequent case regarding vinyl and wax recordings. Motor speed fluctuations can be the reason of wow presence especially in semi-professional cassettes. In case of movies, sound track damages and inappropriate production techniques can trigger wow. Therefore the distortion can be found in the movie soundtracks, where careless cuts and joins of the separate magnetic audio tape, made synchronously with the optical tape, introduce high wow risk.

Wow is very difficult to combat with, especially in the analogue domain. Providentially digital signal processing can be successfully used for wow restoration. Such processing involves two steps. Firstly the wow characteristic determination and secondly the compensation. Details on wow determination can be found in author's previous papers [2-5] whereas this paper address the compensation problem. The presented approach involves a resampling method with a chosen interpolation technique.

The organization of the paper is the following. Section 2 defines the wow defect and presents characteristics useful in

wow reduction. Section 3 depicts different interpolation techniques utilized in experiments. Main results are reported in Section 4, followed by conclusions.

2. Wow definition and characteristics

The irregular motion of the recording medium introduces an undesired frequency modulation (FM) into the signal. This results in such forms of distortions as: drift, wow, flutter and FM noise [6]. Each of them is a FM of the signal, characterised by a different frequency range, leading to a different perception. Drift is a FM in the range below approximately 0.5 Hz, resulting in a distortion perceived as a slow changing of the average pitch. Wow is a FM in the range from approximately 0.5 to 6 Hz, perceived as a fluctuation of pitch. Flutter is a FM in the range from approximately 6 to 100 Hz, causing roughening of the sound quality. FM noise is a FM in the range above 100 Hz, perceived as a noise added to the signal. Hereafter we shall focus on the wow defect exclusively.

The wow defect can be described by using a time warping function $f_w(t)$. It characterizes the wow defect as a distortion of the time axis t of the original signal $x(t)$. Because the sound conveyer playback velocity may be different from that used in recording, the function $f_w(t)$ represents the time axis changes relatively to the original recording. Consequently the distorted signal $x_w(t)$ can be written as

$$x_w(t) = x(f_w(t)). \quad (1)$$

The time warping function is a mapping of the original time axis t to the distorted time axis $f_w(t)$, as presented in Fig. 1.

The second, commonly used, wow characteristic is a *pitch variation function* $p_w(t)$. This function describes the parasite FM caused by the irregular playback and is closely connected to the standard wow definition [6]. There exists the following

*e-mail: p_maziewski@pg.gda.pl

relation between the two functions: f_w and p_w :

$$p_w(t) = \frac{df_w(t)}{dt}. \tag{2}$$

If the pitch is constant, i.e. there is no wow, the p_w equals one. Deviations from unity illustrate the pitch variations and indicate the depth of the wow defect. In most real-life recordings the p_w is close to a constant unity function with seldom varying parts indicating wow.

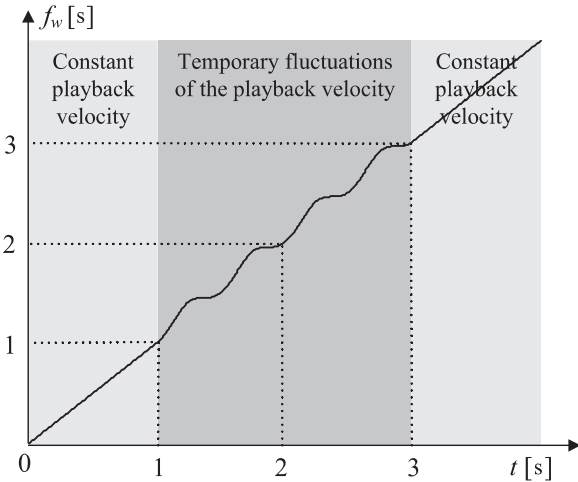


Fig. 1. An example of the time warping function $f_w(t)$

Both characteristics, i.e., p_w and f_w , can be computed utilizing different algorithms for wow evaluation. Details on wow evaluation can be found in papers [2–5].

Based on the distorted signal and the pitch variation function (or equivalently on the time warping function) one can attempt to reduce wow. Further on the wow reduction is performed by non-uniform sampling rate conversion, on the basis

of the wow characteristic, and utilizing different interpolation techniques.

3. Wow reduction based on different interpolation techniques

Utilizing either the pitch variation curve p_w or the time warping function f_w it is possible to recover the original, undistorted signal. Equation 3 presents the formula for the restored signal.

$$x_{rec}(t) = x_w(f_w^{-1}(t)) \cong x(t). \tag{3}$$

When dealing with the discrete-time signals, assuming constant playback velocity, the sampling interval width T is considered to be fixed and constant. However, in case of a variable velocity of the sound conveyer, i.e., wow presence, the sampling instants can be considered as irregularly spaced. This occurs irrespectively of the constant sampling interval T of the analogue-to-digital converter. Thus, in the digital time domain, wow can be seen and characterised as having a time-varying sampling interval width $T_w[n]$. The T_w can be derived from the defect characteristics such as the discrete forms of the time warping function $f_w[n]$ or the pitch variation function $p_w[n]$

$$T_w[n] \cong f_w[n] - f_w[n - 1]. \tag{4}$$

The T_w symbolizes the distorted time axis which should be corrected. Utilizing the irregularly spaced sound samples $x_w(T_w[n])$ and the wow characteristic, e.g. $p_w[n]$, the original signal can be reconstructed. To achieve this, the width $T_{dw}[n]$ of the new sampling instants, defined regarding the distorted time axis T_w , must be computed. Based on Eq. 3 and the property of inverse functions, i.e. the f_w^{-1} is symmetrical to f_w relatively to the line $y = x$, the following equation can be written:

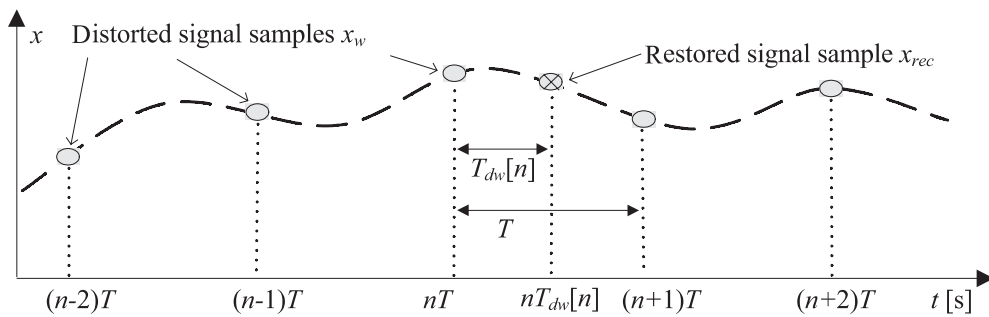


Fig. 2. An illustration of the idea of signal restoration using non-uniform interpolation

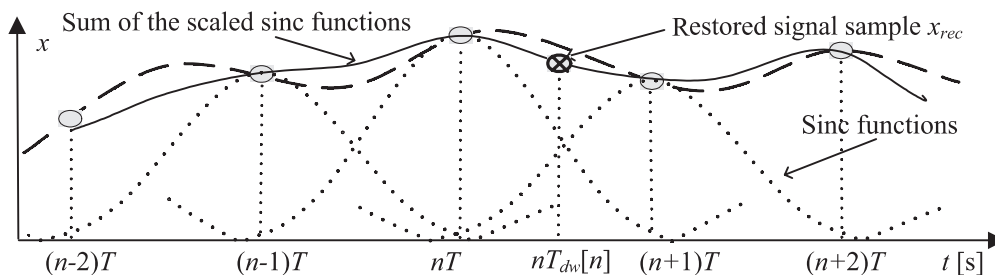


Fig. 3. Restoring a sample based on the sinc-based interpolation technique

$$T_w[n] \cdot T_{dw}[n] = T. \quad (5)$$

Further on, basing on Equations 2, 4 and 5, the following formula for the restored sampling interval width can be given:

$$T_{dw}[n] = \frac{T}{p_w[n]}. \quad (6)$$

This equation shows, that reconstruction of the original signal can be interpreted as an interpolation of non-uniformly spaced signal samples, $x_{rec}[n] \cong x[n]$. Such a process will utilize the distorted time axis and signal values as well; see Fig. 2 for graphical interpretation.

In the following a short overview of the interpolation techniques used further in experiments is presented.

3.1. Sinc-based interpolation. The sinc-based interpolation of irregularly spaced samples is the one most closely connected with the Shannon sampling theorem. In this method the equation used to obtain the sample $x(nT_{dw})$, delayed by the amount $T_{dw} > 0$ (see Eq. (6)) relative to $x_w(nT)$, is given by Eqs. 7 and 8 [7].

$$x_{rec}(nT_{dw}) = \sum_{m=-N/2}^{N/2} x_w(mT) \cdot h\left(\frac{nT_{dw}}{T} - m\right) \quad (7)$$

$$h(t) = \gamma \cdot \text{win}(t) \text{sinc}(\gamma \cdot t). \quad (8)$$

In Eq. 7 the n -th value $x(nT_{dw})$ is a sum of the nearest N neighbours on both its sides. The factor γ in Eq. 8 is a number given by the minimum of number 1 and the current sampling rate conversion factor T/T_{dw} . The win function in Eq. 8, whose choice is crucial for the accuracy of interpolation, represents the time domain function for sinc windowing. Details on this method can be found in [7].

An illustration of the sinc-based interpolation is given in Fig. 3. Notice that the restored signal is build as a sum of scaled sinc functions.

3.2. Polynomial-based interpolation. Basing on given N signal values an interpolating polynomial of degree $N - 1$ can be created. Such a function allows computation of the restored samples. The simplest form of the polynomial processing is the linear interpolation. It involves only 2 distorted signal values ($N = 2$). It can be interpreted as joining two neighbouring signal samples by a straight line and returning the signal value along that line at an appropriate instant of time nT_{dw} . The main drawback of this method is that it is a very rough type of interpolation. However, it will be used further in the experiments for the comparison purposes, because of its simplicity and low computational cost. Fig. 4 presents a graphical interpretation of this method.

More generally, a higher order interpolating polynomial can be applied in wow reduction. Such polynomial can be written by using the classical Lagrange formula, originally proposed in [8]. The main advantage of higher order polynomials is due to their abilities of generally more precise interpolation. Thus obtained results are expected to be more accurate.

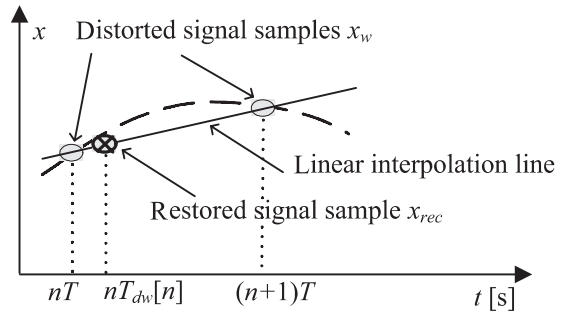


Fig. 4. Restoring a sample using linear interpolation

3.3. Cubic and Spline interpolation. Despite the Lagrange interpolation there exist other, more sophisticated, polynomial-based interpolation methods. One of them is the piecewise cubic Hermite interpolation. The idea of this approach is the following [9]:

- On each subinterval $\langle (n - N)T, nT \rangle$, a cubic Hermite interpolating polynomial $P(t)$ is created. It interpolates x_w values such that, at a set of nodes $t = nT$, the polynomial gives a precise signal values $P(nT) = x_w(nT)$.
- $P(t)$ interpolates the signal in a way that the first derivative $P'(t)$ is continuous. However, the second derivative $P''(t)$ is not necessarily continuous. Therefore jumps at the nodes $t = nT$ may occur.
- The slopes at the nodes $t = nT$ are chosen in such a way that $P(t)$ preserves the shape of the data and respects monotonicity. This means that on intervals where the data are monotonic, so is the $P(t)$, and at points where the data have a local extreme, so does the $P(t)$.

Another variant is the cubic spline interpolation. Here the interpolation polynomial is constructed in almost the same way as the Hermite one. However, spline chooses the slopes at $t = nT$ nodes differently, in order to make the $P''(t)$ continuous. This has the following effects [10]:

- Spline produces a smoother result, i.e. $P''(t)$ is continuous.
- It produces a more accurate result if the data consist of values of a smooth function.

Both polynomial based methods, Hermitian and spline, are equally numerically expensive. In the experiments the 3rd order polynomials were used. Therefore four distorted samples ($N = 4$) were involved in the computation of each restored sample.

3.4. Polynomial filtering with additional noise reduction.

The wow defects can be found especially in old archival recordings. Those are most often harmed by additional noise. Therefore a method for wow cancellation and simultaneous noise reduction can be very useful. A polynomial based approach to this problem was presented by T.I. Laakso, A. Tarczynski, N.P. Murphy and V. Valimaki. In [11] it was assumed that a signal is contaminated by a wideband noise which should be lessened in the non-uniform resampling process. This means a statistically-based method. Two models for non-uniformly spaced time axes were given in [11]. One of them,

i.e., additive random resampling, can be directly utilized as a wow reduction scheme. Therefore it was engaged in the following experiments. Details on this method can be found in [11]. In the experiments overview, given in the following section, this method will be referred as ‘Polynomial + NR’.

4. Experiments

This section describes the evaluation method and the obtained results. The proposed method was built to compare different interpolation techniques, utilizing standard audio distortion measures. The signals used in the experiments were artificially prepared using wow characteristics which holds all of the properties used when deriving formulas (3) to (6).

4.1. Wow simulation. As wow can be defined as a parasite FM (see Section 2), one of the simplest defect simulations is a sweep tone x_w with a variable (modulated) instantaneous frequency $f(t)$:

$$x_w = \cos(2\pi f(t)t + \phi_0) \tag{9}$$

where ϕ_0 is the initial phase.

The $f(t)$ can be defined using the pitch variation function $f(t) = f_0 p_w(t)$. The f_0 is the initial instantaneous frequency. Here the $p_w(t)$ represents the FM introduced to the x_w signal. An exemplary sweep tone, with a linearly increasing instantaneous frequency, i.e., $p_w(t) = t + 1$, was used during the experiments (see Fig. 5). Such a signal simulates the effect of linearly increased speed of the recording medium (i.e. wow signal x_w).

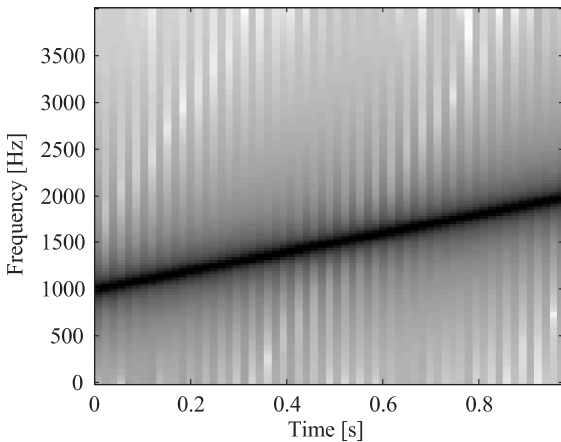


Fig. 5. A sweep tone – an exemplary simulation of the wow defect

In case of such a FM tone (Fig. 5), the wow reduction requires non-uniform sampling rate conversion to obtain an unmodulated signal, i.e., a tone with a constant instantaneous frequency. This steady tone, representing the restored signal x_{rec} , would be obtained if the speed of the recording medium was constant at the beginning.

The following figures present the resampled signals utilizing the cubic Hermitan method (Fig. 6) and the windowed sinc-based method (Fig. 7). Comparing Figs. 5, 6 and 7, one can notice the time length difference between the ‘wowed’ and ‘de-wowed’ signals. It is due to the cancellation of the simulated speed increase of the recording medium.

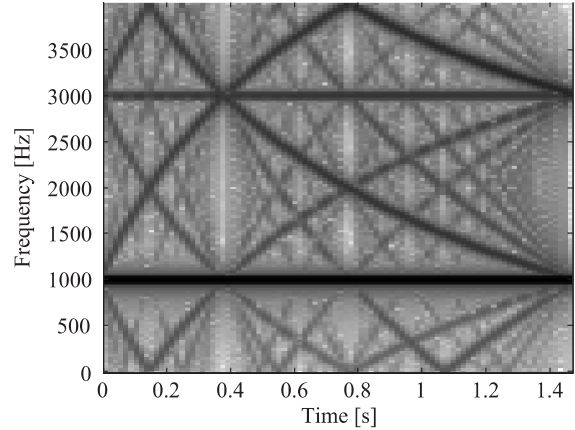


Fig. 6. A steady tone – simulated signal with removed wow defect using the cubic ($N = 4$) Hermitan method

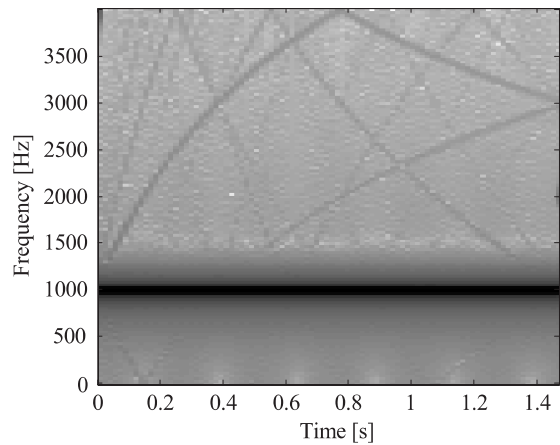


Fig. 7. A steady tone – simulated signal with removed wow defect using the windowed sinc-based method with long von Hann window

The results obtained using the cubic Hermitan method involved 3rd order interpolation, thus with $N = 4$.

In case of the sinc-based method, the von Hann window was used and the interpolation order was 200 ($N = 201$).

On both spectrograms different distortions, introduced by the resampling process, can be noticed.

4.2. Evaluation of wow reduction methods. As can be noticed on the preceding spectrograms, the resampling processes introduces distortions into the signal. An examination of the distortions can be performed on the basis of the amplitude spectrum. Therefore, Fig. 8 presents amplitude spectra of the two restored signals, from Figs. 6 and 7. To visualize the level of the distortions better, also the amplitude spectrum of an undistorted (unprocessed) tone with a steady instantaneous frequency was shown. The vertical axis of the chart is given in full scale decibels (dBFS) which are normalized dB units (the same as the dBc in case of pure tone signals). The horizontal axis is given in frequency bins (4096 point DFT was utilized to compute spectra).

It can be seen in Fig. 8 that both of the restored signals have higher, and variable, noise floor levels, comparing to the gene-

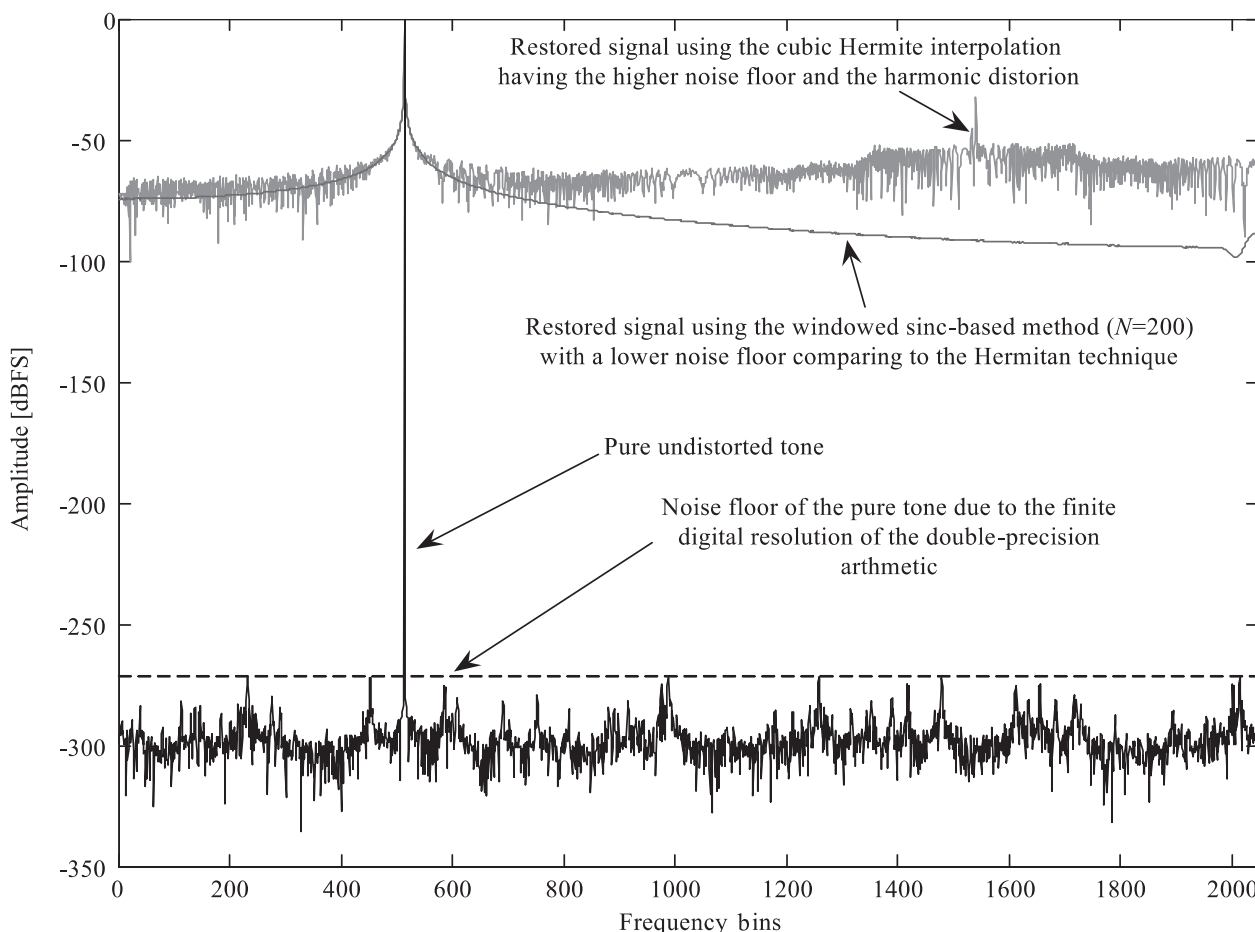


Fig. 8. Amplitude spectra of two signals restored by the windowed sinc-based method with the von Hann window and the polynomial-based cubic Hermitan method, and the spectrum of a tone undistorted by wow

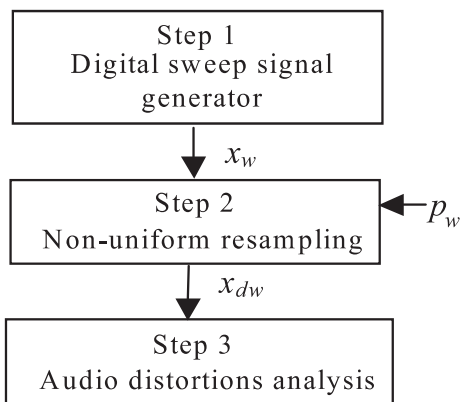


Fig. 9. Block diagram of processing for a comparison between different resampling methods aimed at the wow reduction

ric tone without wow. It is due to the interpolation kernel influence caused by the side lobes of its spectrum. The maximal value of the kernel spectrum side lobes decreases with a higher interpolation order. For details on kernels influence see [12].

The other audio distortion, presented in Fig. 8, is exposed by the signal spectrum restored with the cubic Hermite method. It is the parasite 3rd harmonic introduced by the

resampling process (also visible on the spectrogram in Fig. 6). This indicates that some of the interpolation techniques can introduce non-linear distortions.

The analysis of the amplitude spectrum revealed two main types of distortions influencing the restored signal quality. Those are: the variable noise floor and different nonlinearities. To assess the distortions three standard audio quality measures were chosen [13]:

Total Harmonic Distortion (THD) – defined as the ratio of the harmonic power (HP) to the fundamental frequency power (FFP). This descriptor is given by the following formula :

$$THD = \frac{\sqrt{H_2^2 + H_3^2 + \dots + H_N^2}}{\sqrt{H_1^2 + H_2^2 + H_3^2 + \dots + H_N^2}} \cdot 100\% \quad (10)$$

where H_2, \dots, H_N are the powers of the harmonics, and H_1 is the power of the fundamental (pure) tone

The THD was computed by searching over the entire spectrum to find the peak (fundamental) frequency and then calculating the total power in the harmonic frequencies. The THD is then computed as the ratio of the total HP to the FFP. Residual noise is not included in this calculation.

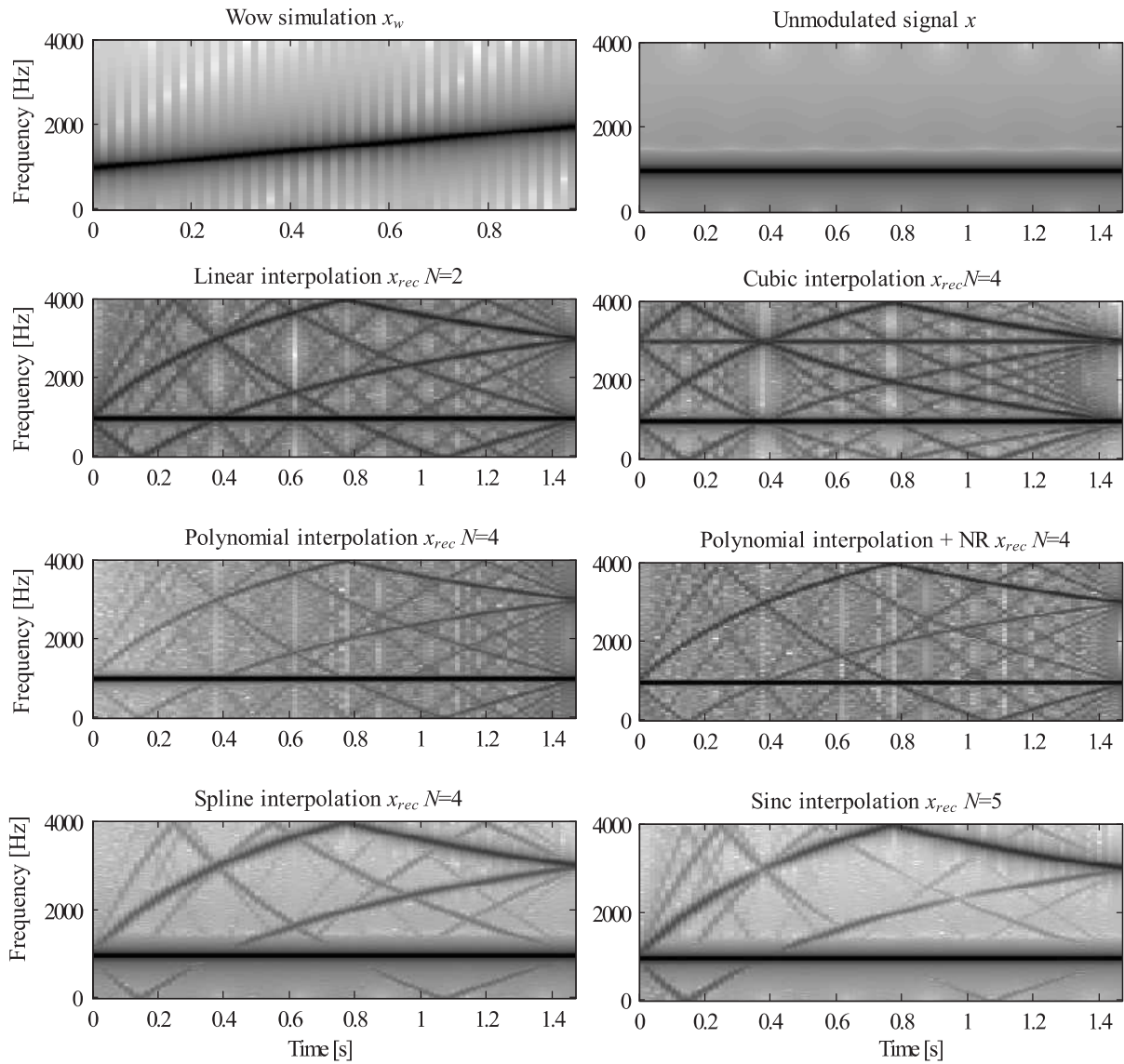


Fig. 10. Spectrograms of the signals without noise at the output of step 2 (see Fig. 9) with short interpolators

Table 1

Audio distortion measures for the undistorted sweep tone resampled utilizing the investigated interpolation methods involving less than 5 samples

Audio distortion measure	'Short' interpolation					
	Linear ($N = 2$)	Polynomial ($N = 4$)	Polynomial + NR ($N = 4$)	Cubic ($N = 4$)	Spline ($N = 4$)	Windowed sinc with the von Hann window ($N = 5$)
THD [%]	0.070147	0.024071	0.232512	0.065450	0.006603	0.012736
THD+N [%]	0.163958	0.070951	0.328568	0.155821	0.084552	0.086483
SNR [dBFS]	62.832	75.852	56.147	63.931	79.483	78.850

Table 2

Audio distortion measures for the undistorted sweep tone resampled utilizing the investigated interpolation methods involving more than 20 samples

Audio distortion measure	'Long' interpolation	
	Windowed sinc with the von Hann window ($N = 21$)	Windowed sinc with the von Hann window ($N = 201$)
THD [%]	0.006416	0.006419
THD+N [%]	0.083799	0.083800
SNR [dB]	80.822	80.823

Table 3

Audio distortion measures for the noised sweep tone resampled utilizing the investigated interpolation methods involving less than 5 samples

Audio distortion measure	‘Short’ interpolation					
	Linear ($N = 2$)	Polynomial ($N = 4$)	Polynomial + NR ($N = 4$)	Cubic ($N = 4$)	Spline ($N = 4$)	Windowed sinc with the von Hann window ($N = 5$)
THD [%]	1.326110	1.580832	0.719541	1.521003	1.558925	1.445902
THD+N [%]	1.520355	1.783527	0.926815	1.712299	1.745984	1.639038
SNR [dBFS]	45.047	43.775	47.692	44.311	44.542	44.638

Table 4

Audio distortion measures for the noised sweep tone resampled utilizing the investigated interpolation methods involving more than 20 samples

Audio distortion measure	‘Long’ interpolation	
	Windowed sinc with the von Hann window ($N = 21$)	Windowed sinc with the von Hann window ($N = 201$)
THD [%]	1.654525	1.656755
THD+N [%]	1.846925	1.857568
SNR [dB]	44.266	43.986

Total Harmonic Distortion plus Noise (THD+N) – defined as the ratio of the HP plus noise, to the FFP. It can be given as:

$$THD + N = \frac{\sqrt{H_2^2 + H_3^2 + \dots + H_N^2 + s^2}}{\sqrt{H_1^2 + H_2^2 + H_3^2 + \dots + H_N^2 + s^2}} \cdot 100\% \quad (11)$$

where s stands for the noise power level. The THD+N was computed in a similar manner as the THD, by searching over the entire spectrum to find the peak (fundamental) frequency and then calculating the total power in the remaining spectrum (harmonics plus noise here). The THD+N level was then computed as the ratio of the total HP plus noise power to the FFP.

The Signal to Noise Ratio (SNR) – the ratio of the signal peak power to the total noise power. The SNR was computed by searching over the entire spectrum to find the peak frequency and then calculating the total noise power in the remaining spectrum.

4.3. Measurements method and results. Figure 9 presents the block diagram of the processing used hereafter for the evaluation and comparison of the effectiveness of different resampling routines considered in Section 3.

The evaluation method is based on three processing steps. In step 1 a synthetic audio signal x_w is generated. During the experiments, two signal versions were used: a pure undistorted sweep tone (see Eq. 9), and the same sweep tone contaminated by an additive wideband noise (the white noise with -43 dBFS level). The latter signal version was necessary to evaluate the effectiveness of the interpolation method with the additional noise reduction mentioned in Section 3.4. The instantaneous frequency of the sweep tone was varied from $f_0 = 1001.2939$ Hz to $f_1 = 2f_0$. The starting frequency f_0 was chosen to minimize the spectral leakage in the 4096 point DFT applied in order to compute the audio distortions’ measures. Both signal’s versions were build at 8 kHz sampling rate.

There were two reasons for choosing these frequency val-

ues. Firstly, the relation of the signal frequency to the sampling rate allows the signal spectrum to overlap only in a quarter of the signal bandwidth. Therefore the distortions generated by the investigated interpolation methods are clearly seen on the spectrograms – see Figs. 6, 7 and 10. Secondly, the resampling routine generates a tone whose frequency f_0 is well suited to the needs of the audio distortion measurements.

The second processing step in Fig. 9 activates one of the investigated interpolation algorithms (see Sect. 3). The signal x_w is non-uniformly resampled utilizing the pitch variation function $p_w(t)$ (see Eq. 9 and the following paragraph), to obtain the output x_{dw} whose FM is reduced. Thus in step 2 the output signal should have a constant instantaneous frequency f_0 as above. It constitutes an input for step 3 – the audio distortion analysis block where three standard audio distortion measures, defined in Sect. 4.2, were applied.

Figure 10 presents spectrograms of the signals x , x_w and x_{dw} obtained using the examined interpolation techniques. In the figure upper left corner, the spectrogram of the simulated wow signal x_w is presented. Then the spectrogram of the unmodulated signal x , symbolizing the restoration goal $x_{rec} = x$, is plotted in the upper right part of the figure. Different time lengths of both signals can be noticed. The wowed signal is shorter due to the simulated speed increase of the recording medium.

In the figure’s next rows, the spectrograms of the restored signal x_{rec} , obtained using different interpolation techniques, are plotted. Engaged are: the first order linear interpolation ($N = 2$), fourth order polynomial-based methods ($N = 4$) including the technique with additional noise reduction, i.e., Polynomial+NR, and the short ($N = 5$) windowed sinc-based method involving the von Hann window. For the convenience spectrogram from Fig. 6 is also presented in Fig. 10. Different distortions, caused by different methods, can be observed in Fig. 10. These distortions’ measures are given in the Tables 1–4.

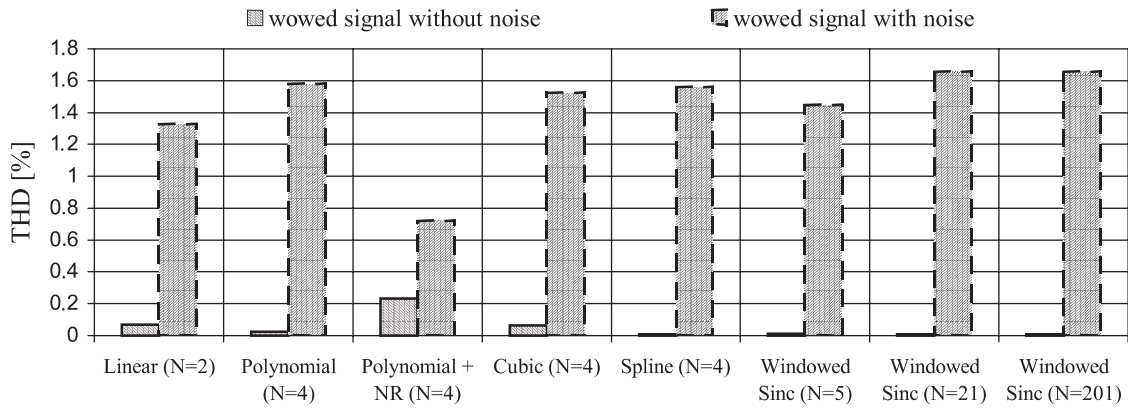


Fig. 11. THD levels for both wowed signals with and without additional noise restored utilizing all the investigated interpolation techniques

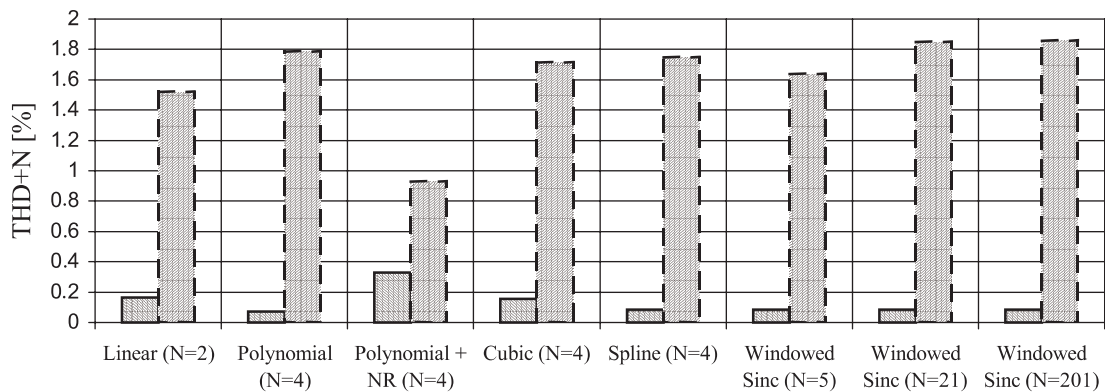


Fig. 12. THD+N levels for both wowed signals with and without additional noise restored utilizing all the investigated interpolation techniques

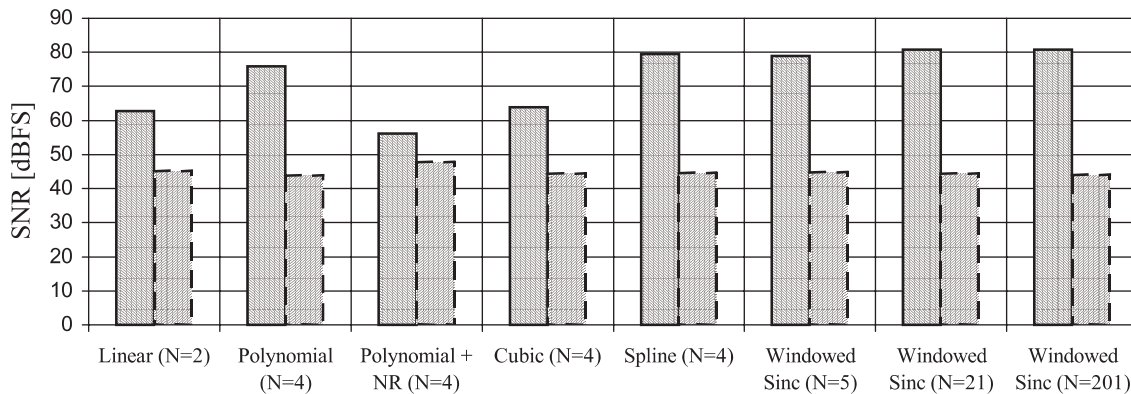


Fig. 13. SNR levels for both wowed signals with and without additional noise restored utilizing all the investigated interpolation techniques

The results gathered in the tables are divided into two groups. The distortion measures obtained for the sweep tone without noise are given in Tables 1 and 2. Tables 3 and 4 give results for the noisy sweep tone. The results of ‘short’ interpolation techniques, given in Tables 1 and 3, involved no more than 5 neighbouring samples for one output sample computation. Namely, in linear interpolation, $N = 2$ neighbouring input samples are used for one output sample computation, while in the cubic, spline and other polynomial techniques $N = 4$ samples, and in the ‘short’ sinc-based method $N = 5$ samples are involved.

The ‘long’ interpolation results, presented in Tables 2 and 4, were obtained using the windowed sinc-based technique with more than $N = 20$ samples involved. In the experiments the von Hann window was used.

To visualise the obtained results better additional charts are presented. Figs. 11–13 give plots of the data from the preceding tables. Fig. 11 depicts the THD for the wowed signal with and without additional noise, restored utilizing all the above mentioned interpolation techniques. Fig. 12 presents the THD+N whereas Fig. 13 illustrates the SNR.

In case of pure sweep tone processing, the results gath-

ered in Tables 1 and 2 indicate that for the ‘short’ interpolation the spline and the windowed sinc-based technique are the most suitable for wow cancellation. It is visible in Figs. 10–13, that both techniques lead to relatively low THD, THD+N and higher SNR values comparing to the other methods. However, when the number of the samples involved increases, the values of distortions measured for the windowed sinc-based technique decrease and become smallest here – see ‘long’ interpolation results in Table 2 and SNR values in Fig. 13. Obviously, the computation time becomes much longer than for the ‘short’ interpolation techniques.

For the windowed sinc-based technique the number N of samples involved in interpolation is very important to achieve the desired high SNR. However, after reaching a certain point, e.g., $N = 21$, increasing the number of samples does not bring any significant improvements – see Tables 2 and 4, and Fig. 12.

In case of noised signal, see Tables 3 and 4, the polynomial processing, with additional noise reduction, was found to be most successful. This is also noticeable in Figs. 10 and 11, where the THD is lowest and the SNR is highest. The gained advantage is 3dB in SNR and almost a half amount of THD, comparing to the windowed sinc-based method.

5. Conclusions

In the paper different resampling methods were examined. The results obtained using a sweep tone without noise indicate that, in terms of the chosen audio distortion measures, the windowed sinc-based method, involving more than 20 samples, was the best. Its main disadvantage was only the long computation time, but because the reduction of the wow defect can be performed offline, the computation time is not that important. In this light the ‘long’ sinc-based interpolation technique seems to be the most appropriate one for wow reduction, expressed in terms of low audio distortions’ levels.

Concerning the noised sweep tone, the polynomial filtering, with additional noise reduction, was found very promising. Its main advantage is due to the gained SNR and low THD and THD+N.

Acknowledgments. This work was supported by the Commission of the European Communities, Directorate-General of the Information Society under the Integrated Project No. FP6-507336 entitled: “PRESTOSPACE – Preservation towards storage and access. Standardized Practices for Audiovisual Contents Archiving in Europe”.

REFERENCES

- [1] G. Brock-Nannestad, “What are the sources of the noises we remove?”, *Proc. AES 20th Int. Conf.* 1960, (2001).
- [2] A. Czyzewski, P. Maziewski, M. Dziubinski, A. Kaczmarek and B. Kostek, “Wow detection and compensation employing spectral processing of audio”, *Proc. 117 AES Conv.* 6212, (2004).
- [3] A. Czyzewski, M. Dziubinski, A. Ciarkowski, M. Kulesza, P. Maziewski and J. Kotus, “New algorithms for wow and flutter detection and compensation in audio”, *Proc. 118 AES Conv.* 6353, (2005).
- [4] A. Czyzewski, P. Maziewski, M. Dziubinski, A. Kaczmarek, M. Kulesza and A. Ciarkowski, “Methods for detection and removal of parasitic frequency modulation in audio recordings”, *Proc. AES 26th Int. Conf.* 3–3, (2005).
- [5] A. Czyzewski, M. Dziubinski, L. Litwic and P. Maziewski, “Intelligent algorithms for optical track audio restoration”, *Lecture Notes in Artificial Intelligence* 3642, 283–293 (2005).
- [6] AES 6-1982, “Method for measurement of weighted peak flutter of sound recording and reproducing equipment”, *J. Audio Eng. Soc.* 33 (6), 468–475 (1985).
- [7] F. Marvasti, *Nonuniform Sampling Theory and Practice*, Kluwer Academic Publishers, New York, 2001.
- [8] J.L. Lagrange, “Leçons élémentaires sur les mathématiques données à l’école normale (1795)”, *Oeuvres de Lagrange* 7, Gauthier-Villars, Paris, 183–287 (1877).
- [9] F.N Fritsch and R.E. Carlson, “Monotone piecewise cubic interpolation”, *SIAM J. Num. Analysis* 17, (1980).
- [10] C. de Boor, *A Practical Guide to Splines*, Springer-Verlag, Berlin, 1978.
- [11] T.I. Laakso, A. Tarczynski, N.P. Murphy and V. Valimaki, “Polynomial filtering approach to reconstruction and noise reduction of nonuniformly sampled signal”, *Signal Processing* 80, 567–575 (2000).
- [12] S. K. Mitra, K. Sanjit and J.F. Kaiser, *Handbook for Digital Signal Processing*, John Wiley, 1993.
- [13] B. Metzler, *Audio Measurement Handbook*, Audio Precision, 130–145 (1973).